

VALIDITY REGIONS OF THEORETICAL MODELS FOR ESTIMATING THE RCS OF LOSSY DIELECTRIC CYLINDERS

Jin-Young Hong, Soon-Gu Kwon and Yisok Oh

Department of Radio Science and Communication Engineering, Hongik University, Seoul, Korea
e-mails: nir26@hanmail.net, celldivision@hotmail.com, yisokoh@hongik.ac.kr

ABSTRACT: This paper presents an examination of theoretical scattering models for radar cross sections (RCS) of lossy dielectric cylinders, such as exact analytical solution, low frequency approximation (Rayleigh) and high frequency approximation (Physical Optics). The validity regions of the PO and Rayleigh models are closely examined with exact solution in terms of various wavelengths and dielectric constants of a circular cylinder. And also this paper examines the PO and Rayleigh models for back and forward scatter RCS of a cylinder at various incidence angles and polarizations. It was found that the PO and Rayleigh model have their validity regions for estimating the RCS of a circular cylinder.

KEY WORDS: Lossy dielectric cylinder, RCS, physical optics, Rayleigh, validity regions

1. INTRODUCTION

Trunk and branches are the significant parts of a tree canopy. For remote sensing study of a forested area, electromagnetic scattering of tree trunk and branches are of concern. A simple geometry that best describes branches is a cylinder. The dielectric constant of a branch is high and lossy. Thus a branch may be modelled by a nonmagnetic lossy dielectric cylinder with arbitrary cross section.

At X-band, the diameter of trunk and branches of almost any tree are much larger than the wavelength. The exact analytical solution for estimating RCS of a circular cylinder is commonly used but it is rather complicated and becomes very inefficient when radius of cylinder is large compared with the wavelength. Moreover the computation time is significantly increased. Hence this paper presents an examination of theoretical scattering models, such as exact analytical solution, Rayleigh and PO approximation. And the validity regions of the theoretical models for back and forward scatter RCS are closely examined with exact solution in terms of various incidence angles, polarizations, wavelengths and dielectric constants of a circular cylinder.

2. SCATTERING MODELS FOR A CIRCULAR CYLINDER

2.1 Exact analytical solution

The exact analytical solution for a dielectric cylinder of finite length has been known for a long time (Ruck et al., 1970). This solution is exact as regards to the transverse resonances and assumes the currents on the surface are the same as if the cylinder were infinite in length.

By applying the field equivalence principle and boundary condition, the total electric and magnetic field outside the cylinder region can be attributed to surface currents given by

$$\bar{J}_e = \eta_0^{-1} (\sin \phi' \hat{x}' - \cos \phi' \hat{y}') \cdot \sum_{m=-\infty}^{\infty} (-i)^m \{h_z J_m(x_0) + B_m H_m^{(1)}(x_0)\} e^{im\phi' + ik_0 z' \cos \beta} \quad (1)$$

$$- \frac{\eta_0^{-1}}{ik_0 \sin^2 \beta} \hat{z}' \sum_{m=-\infty}^{\infty} (-i)^m \{k_0 \sin \beta [e_z J'_m(x_0) + A_m H_m^{(1)'}(x_0)] + \frac{im \cos \beta}{\rho} [h_z J_m(x_0) + B_m H_m^{(1)}(x_0)]\} e^{im\phi' + ik_0 z' \cos \beta}$$

$$\bar{J}_m = -(\sin \phi' \hat{x}' - \cos \phi' \hat{y}') \cdot \sum_{m=-\infty}^{\infty} (-i)^m \{e_z J_m(x_0) + A_m H_m^{(1)}(x_0)\} e^{im\phi' + ik_0 z' \cos \beta} \quad (2)$$

$$- \frac{\eta_0^{-1}}{ik_0 \sin^2 \beta} \hat{z}' \sum_{m=-\infty}^{\infty} (-i)^m \{k_0 \sin \beta [h_z J'_m(x_0) + B_m H_m^{(1)'}(x_0)] - \frac{im \cos \beta}{\rho} [e_z J_m(x_0) + A_m H_m^{(1)}(x_0)]\} e^{im\phi' + ik_0 z' \cos \beta}$$

In order to find the scattered fields for a cylinder of finite length $b \gg \lambda_0$, $-b/2 < z' < b/2$, we may assume that the currents on the curved sides are the same as those on the infinite cylinder. If the effect of the end caps is ignored, the Hertz vectors describing the scattered field are

$$\Pi_e(r) = \frac{e^{ik_0 r}}{r} \left(\frac{i\eta_0}{4\pi k_0} \right) \int_{-b/2}^{b/2} \int_0^{2\pi} \bar{J}_e e^{-ik_0 \rho B \cos(\phi' - \tilde{\phi})} e^{ik_0 (\hat{k}_i - \hat{k}_s) \cdot \hat{z}' z'} \rho d\phi' dz' \quad (3)$$

$$\Pi_m(r) = \frac{e^{ik_0 r}}{r} \left(\frac{i\eta_0^{-1}}{4\pi k_0} \right) \int_{-b/2}^{b/2} \int_0^{2\pi} \bar{J}_m e^{-ik_0 \rho B \cos(\phi' - \tilde{\phi})} e^{ik_0 (\hat{k}_i - \hat{k}_s) \cdot \hat{z}' z'} \rho d\phi' dz' \quad (4)$$

where $\tilde{\phi}$ and B are given by

$$B = \left[(\hat{k}_s \cdot \hat{x}')^2 + (\hat{k}_s \cdot \hat{y}')^2 \right]^{1/2} \quad (5)$$

$$\cos \tilde{\phi} = \frac{1}{B} \hat{k}_s \cdot \hat{x}', \quad \sin \tilde{\phi} = \frac{1}{B} \hat{k}_s \cdot \hat{y}' \quad (6)$$

The integration in (1, 2) can be carried out exactly. The z' integration produces $b(\sin V)/V$ with

$$V = \frac{1}{2\pi} k_0 b (\hat{k}_i - \hat{k}_s) \cdot \hat{z}' \quad (7)$$

where $y_0 = k_0 \rho B$. Therefore, the scattering matrix is

$$\bar{S} = \frac{k_0 \rho b}{2 \sin \beta} \left\{ (D^e e_z + i\bar{D}^e h_z) \hat{k}_s \times (\hat{k}_s \times \hat{z}') + (D^h h_z - i\bar{D}^h e_z) \hat{k}_s \times \hat{z}' \right\} \frac{\sin V}{V} \quad (8)$$

with

$$D^e = \sum_{m=-\infty}^{\infty} (-1)^m \left[J_m'(x_0) J_m(y_0) - \frac{\sin \beta}{B} J_m'(y_0) J_m(x_0) + C_m^{TM} \left\{ H_m^{(1)}(x_0) J_m(y_0) - \frac{\sin \beta}{B} H_m^{(1)}(x_0) J_m'(y_0) \right\} + \frac{m \cos \beta}{x_0} \left(1 - \frac{\hat{k}_s \cdot \hat{z}' x_0 \sin \beta}{\cos \beta y_0 B} \right) \bar{C}_m H_m^{(1)}(x_0) J_m(y_0) \right] e^{im\tilde{\phi}} \quad (9)$$

The other elements of scattering matrix in (6) are given by (Ulaby et al, 1990; Sarabandi, 1989).

2.2 Rayleigh approximation

Rayleigh scattering is applied to the case of a homogeneous dielectric cylinder of arbitrary cross section whose transverse dimensions are much smaller than λ_0 . For a plane wave incident obliquely on a cylinder of infinite length, the field can be written as the sum of contributions from line dipoles whose moments per unit length are expressed in terms of polarizability tensors. The electric and magnetic dipole moment per unit length are

$$\bar{p} = \varepsilon_0 (\varepsilon - 1) \left\{ - \int_C (a_x \Phi_1 + a_y \Phi_2) \hat{n}' dc' + Ab_z \hat{z}' \right\} \quad (10)$$

$$\bar{m} = Y_0 (\mu - 1) \left\{ - \int_C (b_x \Psi_1 + b_y \Psi_2) \hat{n}' dc' + Ab_z \hat{z}' \right\} \quad (11)$$

Φ and Ψ are the total electrostatic and magnetostatic potential and \hat{a}, \hat{b} are the unit vectors specifying the directions of the incident electric and magnetic field respectively. The polarizability tensors \bar{P}, \bar{M} are

$$\bar{p} = \varepsilon_0 \bar{P} \cdot \hat{a}, \quad \bar{m} = Y_0 \bar{M} \cdot \hat{b} \quad (12)$$

The far field scattering matrix, defined as the coefficient of $re^{-ik_0 r} E^s$ in the far zone, is then

$$\bar{S} = -\frac{k_0^2}{4\pi} \left\{ \hat{k}_s \times \hat{k}_s \times [l\bar{P} \cdot \hat{a}] + \hat{k}_s \times [l\bar{M} \cdot \hat{b}] \right\} \frac{\sin U}{U} \quad (13)$$

where

$$U = \frac{k_0 l}{2} (\hat{k}_s \cdot \hat{z} - \cos \beta) \quad (14)$$

2.3 Physical optics approximation

The exact analytical solution is rather complicated and becomes very inefficient when radius of the cylinder is large compared with the wavelength. In fact the convergence rate of the series given by (9) is very poor when x_0 and/or y_0 are large. In this case, high frequency approximation with some assumption is available for estimating the RCS of a circular cylinder. At high frequency, each portion of the surface appears locally flat

and the electric and magnetic surface currents are zero on the shadowed region of the surface. This is often referred to as physical optics.

The elements of the scattering matrix are then

$$S_{vv} = - \left\{ R_H (\hat{n}' \cdot \hat{v}_i) (\hat{n}' \cdot \hat{v}_s) + R_E (\hat{n}' \cdot \hat{h}_i) (\hat{n}' \cdot \hat{h}_s) \right\} \frac{\hat{n}' \cdot \hat{k}_i}{\hat{n}' \times \hat{k}_i} Q$$

$$S_{vh} = - \left\{ R_H (\hat{n}' \cdot \hat{h}_i) (\hat{n}' \cdot \hat{v}_s) + R_E (\hat{n}' \cdot \hat{v}_i) (\hat{n}' \cdot \hat{h}_s) \right\} \frac{\hat{n}' \cdot \hat{k}_i}{\hat{n}' \times \hat{k}_i} Q$$

$$S_{hv} = - \left\{ R_H (\hat{n}' \cdot \hat{v}_i) (\hat{n}' \cdot \hat{h}_s) + R_E (\hat{n}' \cdot \hat{h}_i) (\hat{n}' \cdot \hat{v}_s) \right\} \frac{\hat{n}' \cdot \hat{k}_i}{\hat{n}' \times \hat{k}_i} Q$$

$$S_{hh} = - \left\{ R_H (\hat{n}' \cdot \hat{h}_i) (\hat{n}' \cdot \hat{h}_s) + R_E (\hat{n}' \cdot \hat{v}_i) (\hat{n}' \cdot \hat{v}_s) \right\} \frac{\hat{n}' \cdot \hat{k}_i}{\hat{n}' \times \hat{k}_i} Q \quad (15)$$

R_E and R_H are reflection coefficients. The element Q is the integral expression for the illuminated region. Then

$$Q = -\frac{ik_0 \rho}{2\pi} \int_{-b/2}^{b/2} \int_{-\pi/2}^{\pi/2} e^{-ik_0 B \rho \cos(\phi' - \tilde{\phi})} e^{-ik_0 (\hat{k}_i - \hat{k}_s) \cdot \hat{z}' z'} d\phi' dz' \quad (16)$$

$\tilde{\phi}$ and B are defined in (5) and (6). The expression of Q can be simplified using Fresnel integral. then

$$Q = b \sqrt{\frac{k_0 \rho}{2\pi B}} e^{-i(\pi/4) - ik_0 B \rho} \frac{\sin V}{V} \quad (17)$$

The above expressions fail in the forward scattering direction for which $B=0$, but in direction close to forward, an alternative approximation is possible.

$$S \approx -\frac{2ib\rho}{\lambda_0} (\hat{k}_i \cdot \hat{x}') \frac{\sin V}{V} \frac{\sin W}{W} E_0 \quad (18)$$

with

$$W = k_0 \rho (\hat{k}_s \cdot \hat{y}') \quad (19)$$

3. EXAMINATION OF SCATTERING MODELS

In order to examine the validity regions of theoretical models, the length of a cylinder is fixed at 2λ . Then the backscatter and forward-scatter RCSs of a circular cylinder are computed at various incidence angles, dielectric constants and wavelengths. The RCS of a cylinder which its diameter is much larger than wavelength has been usually computed using the physical optics approximation. On the other hand, the RCS of a cylinder which its diameter is smaller than wavelength has commonly been computed using the Rayleigh approximation.

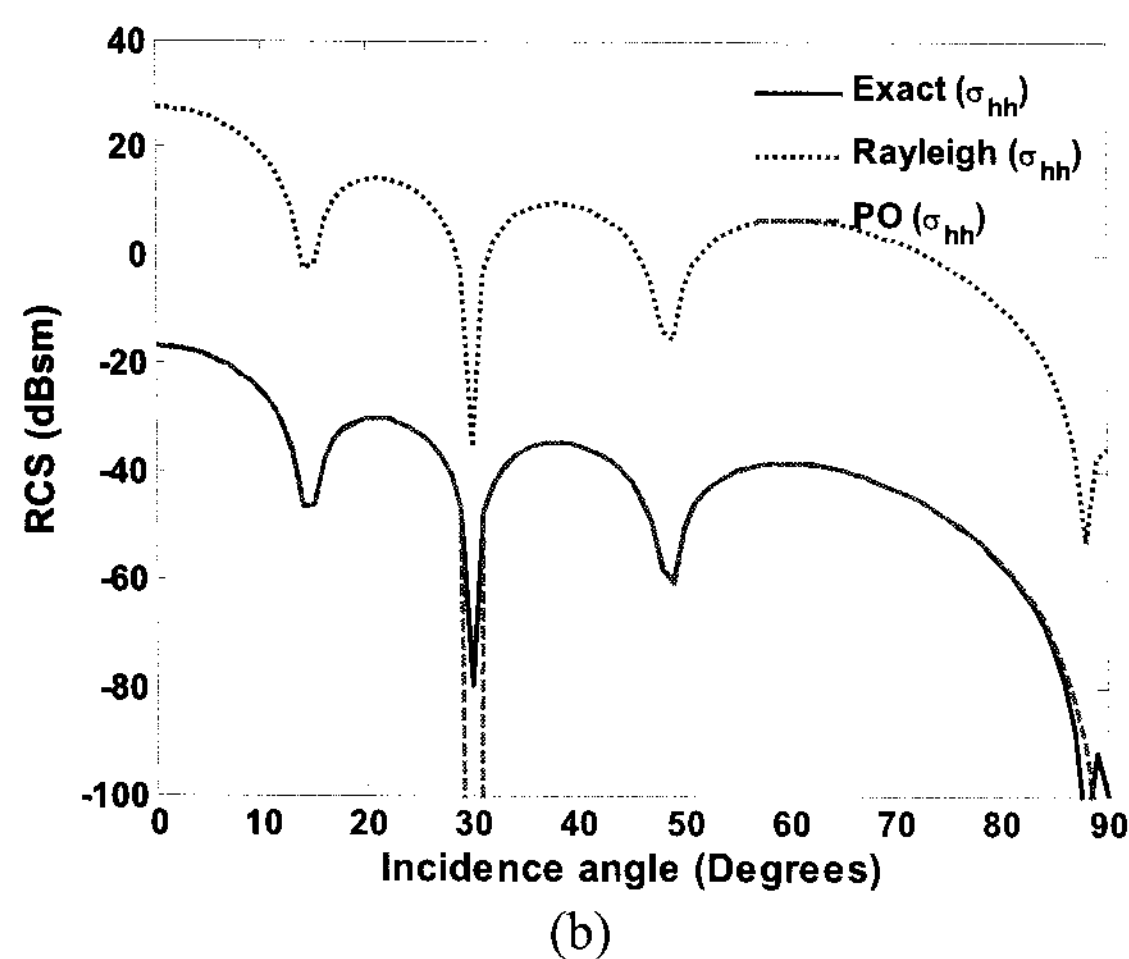
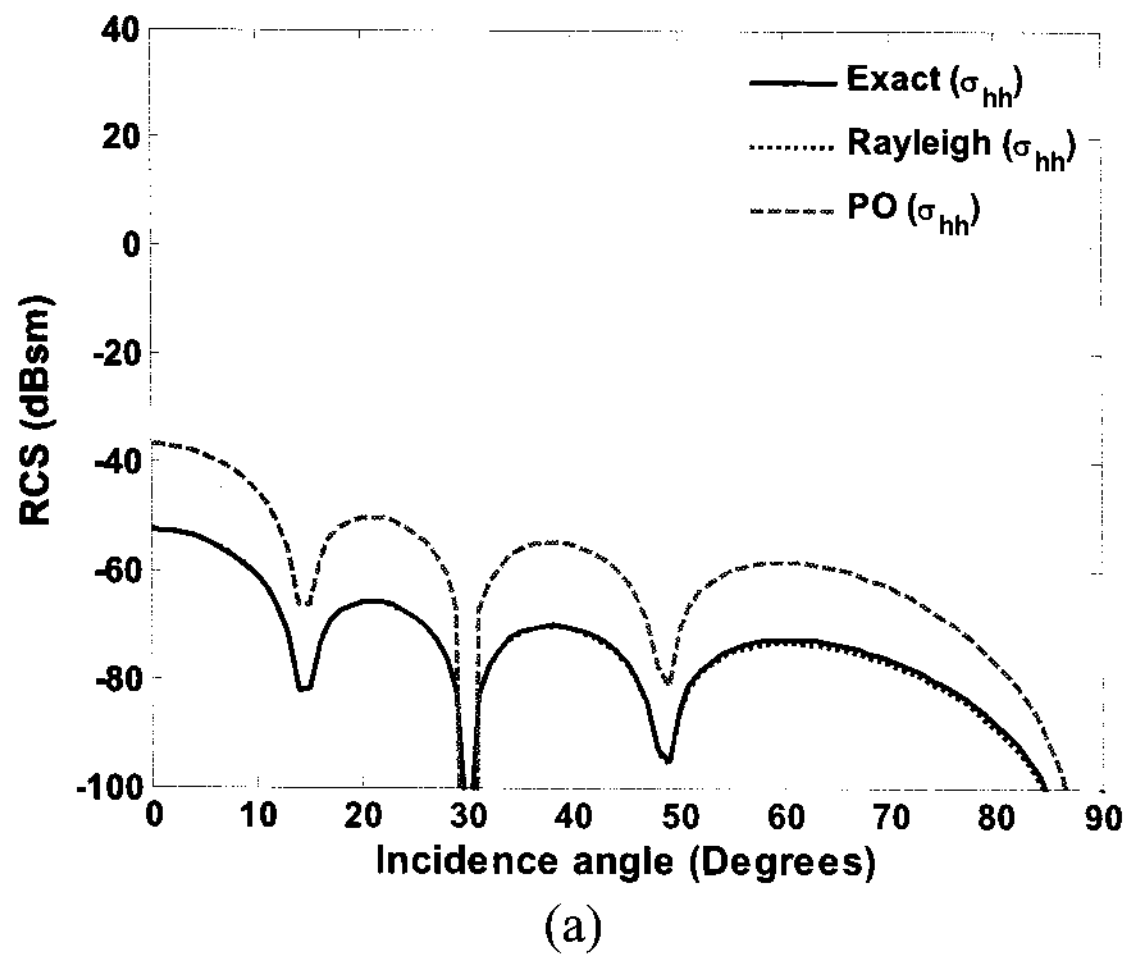


Figure 1. Comparison of the backscatter cross sections for two types of cylinders at various incidence angles (a) cylinder diameter = 0.1λ , (b) 10λ

As expected, figure 1(a) shows that the backscattering RCS of a cylinder using the Rayleigh approximation is exactly same with the exact analytical solution at various incidence angles with a cylinder diameter 0.1λ .

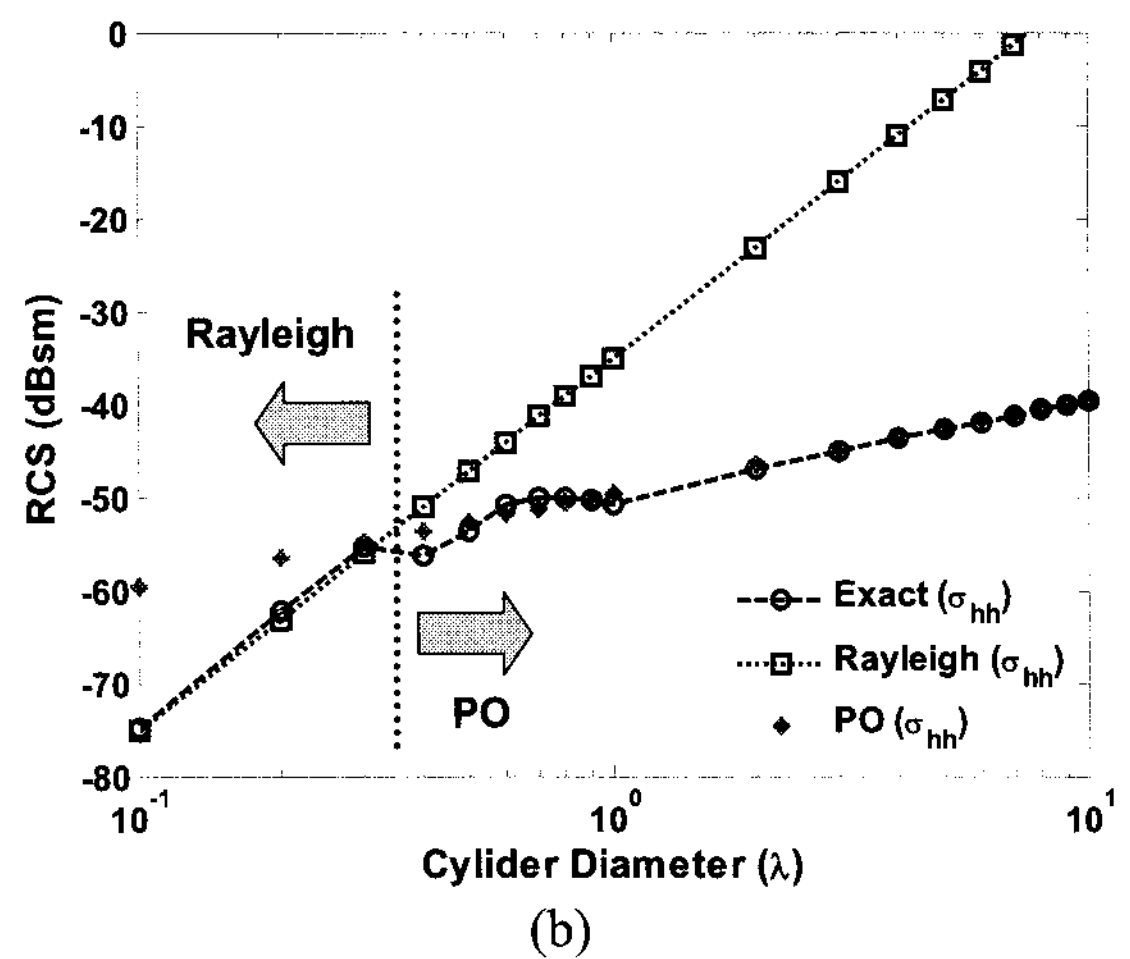
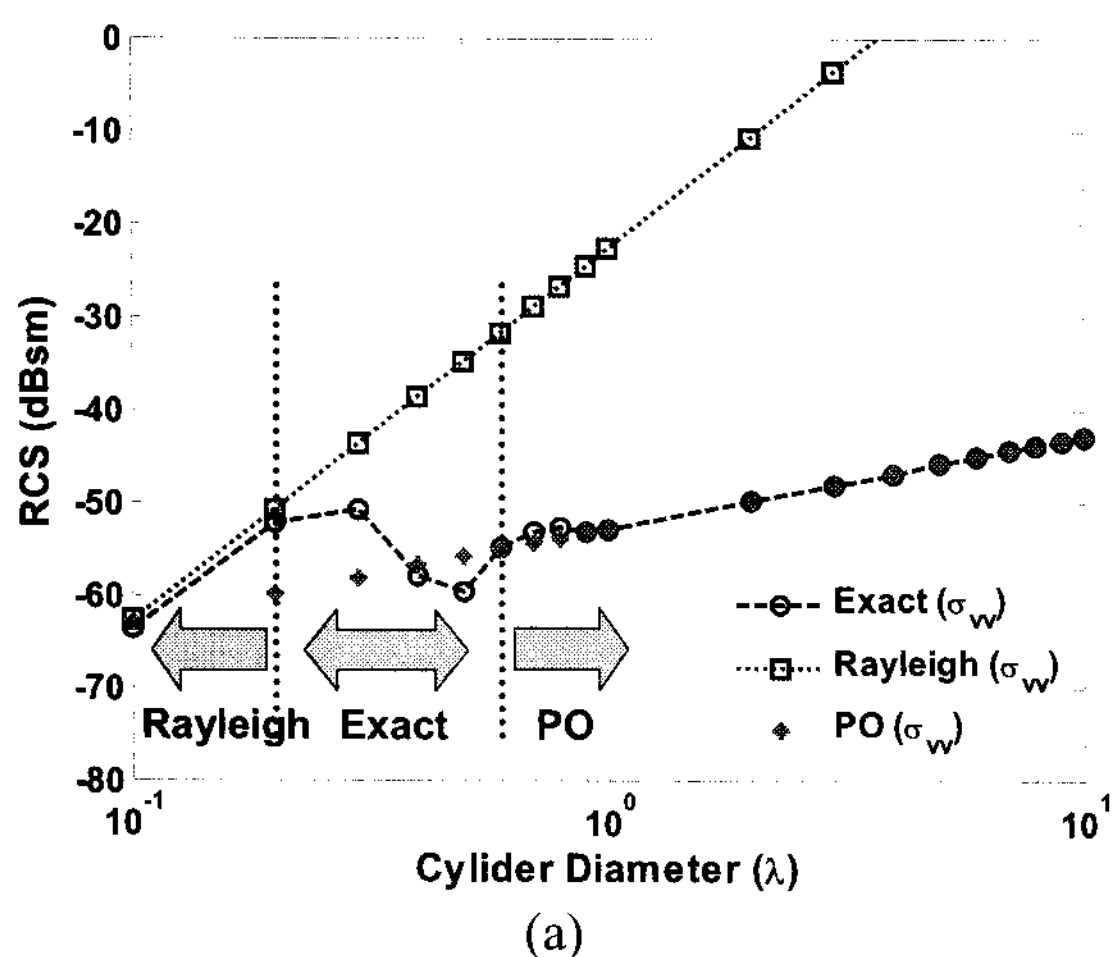
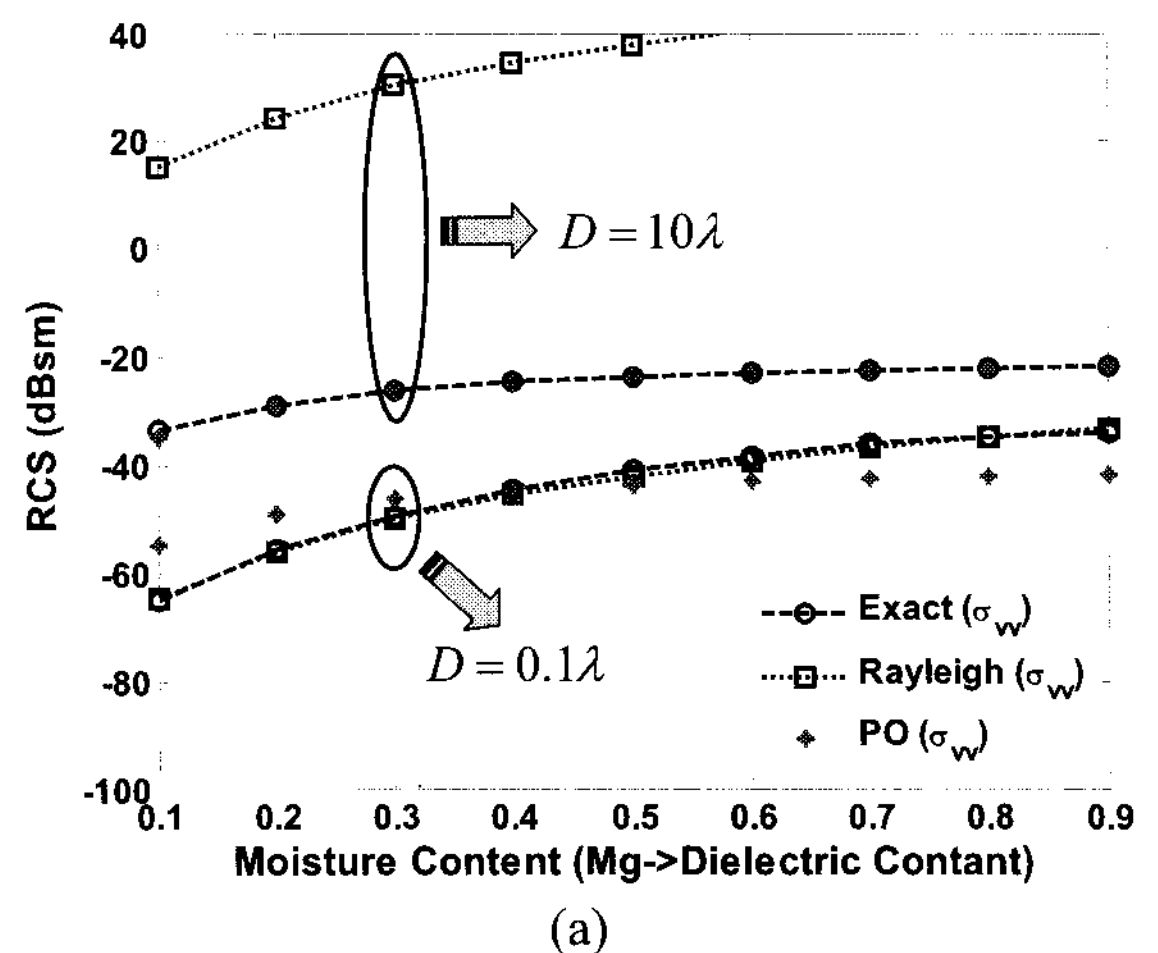


Figure 2. Comparison of the backscatter cross sections as functions of cylinder diameters at 45° incidence angle for (a) vv-, (b) hh-polarization

Figure 1(b) shows that the backscattering RCS of a cylinder using PO approximation is same with the exact solution at a cylinder diameter 10λ .

The first step for the examination of the Rayleigh and PO model is the variation of the backscattering RCS with a function of a cylinder diameter ($0.1 \leq \lambda \leq 10$) for vv- and hh-polarization at 45° incidence angle. Figure 2(a), (b) show that the Rayleigh model is available for a cylinder diameter less than 0.2λ and 0.35λ at vv- and hh-polarization respectively, whereas the PO model agrees well with the exact solution for a cylinder diameter larger than 0.6λ and 0.35λ at vv- and hh-polarization respectively.

The second step for validity regions of theoretical models is the examination of the backscattering RCS with a function of dielectric constant of a cylinder diameter 0.1λ and 10λ . As expected, Figure 3 shows an excellent agreement between Rayleigh and exact analytical solution for a cylinder diameter 0.1λ at vv- and hh-polarization during the variation of dielectric constant.



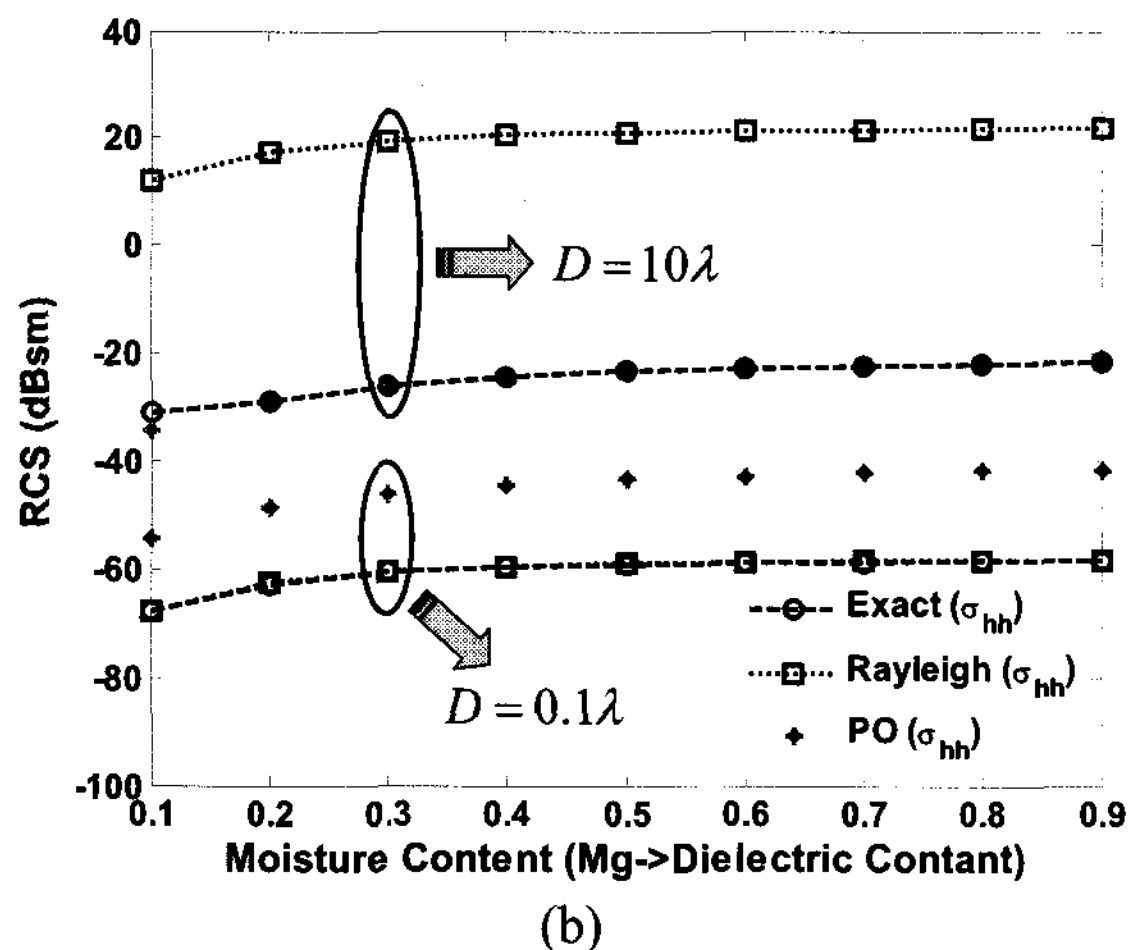


Figure 3. Backscatter RCS as functions of moisture contents (=dielectric constants) of a cylinder at 45° incidence angle (a) vv-, (b) hh-polarization

On the other hand, the PO model agrees quite well with the exact solution for a cylinder diameter 10λ at vv- and hh-polarization during the variation of dielectric constant. The dielectric constants of a branch and/or trunk, corresponding to the gravimetric moisture content of $Mg(g/cm^3)$, are obtained from an empirical formula in (Ulaby et al, 1987). For example, $Mg=0.5g/cm^3$ corresponds to $\epsilon_r=(12.4,-5.2)$ at 9.65GHz.

The third step for the examination of the theoretical models is the variation of the forwardscatter RCS with a function of a cylinder diameter from 0.1 to 10λ for vv- and hh-polarization at 45° incidence angle. Figure 4(a), (b) show that the Rayleigh model is available for a cylinder diameter less than 0.3λ and 0.45λ at vv- and hh-polarization respectively, whereas the PO model agrees well with the exact solution for a cylinder diameter larger than 0.8λ and 0.45λ at vv- and hh-polarization respectively. We could also obtain similar results for the back and forward RCS of a cylinder with different incidence angles, dielectric constants, cylinder diameters and cylinder lengths.

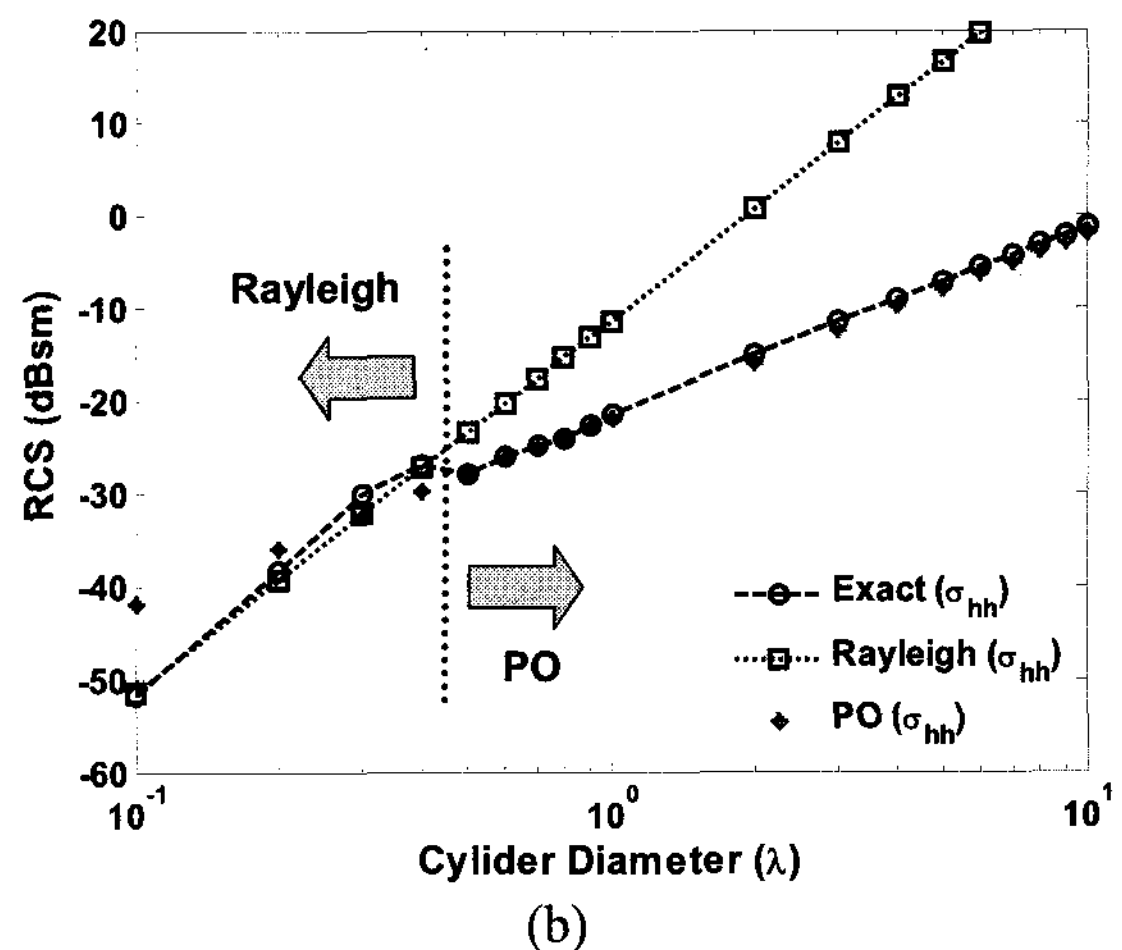
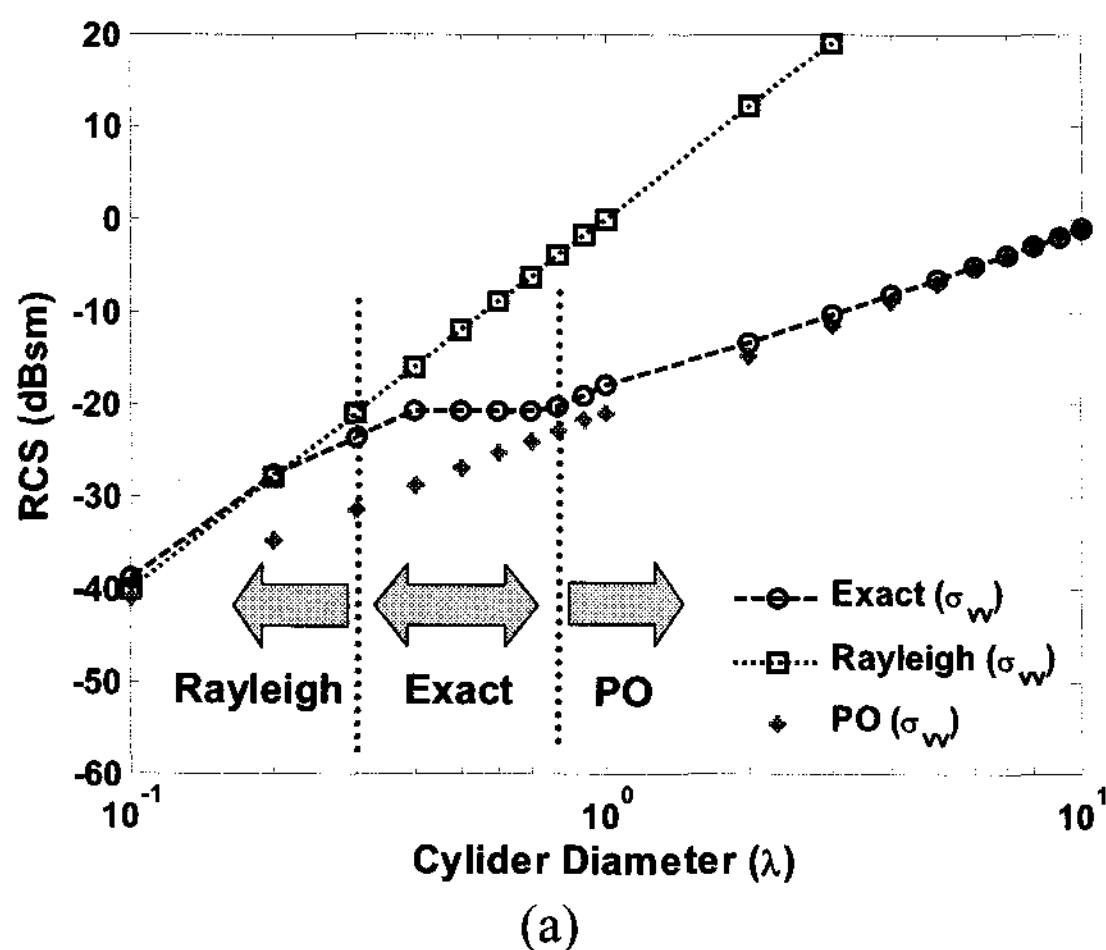


Figure 4. Comparison of the forward-scatter cross sections as functions of cylinder diameters for vv- and hh-polarizations (a) cylinder diameter = 0.1λ , (b) 10λ

4. CONCLUDING REMARKS

The validity regions of the PO and Rayleigh models are closely examined with exact analytical solution for back and forward RCS of a circular cylinder in terms of various wavelengths, incidence angles, polarizations and dielectric constants. As expected, the Rayleigh model is available for estimating the RCS when the diameter of cylinder is small compared with the wavelength. Whereas PO model is available for estimating the RCS when the diameter of cylinder is large compared with the wavelength. The validity regions of the PO and Rayleigh model are slightly different for the polarizations and incidence angles. The exact analytical solution is rather complicate and becomes very inefficient when radius of the cylinder is large compared with the wavelength. Moreover the computation time is significantly increased in accordance with increasing diameter of cylinder. Therefore we can conclude that the PO model is applicable to the computation of the scattering matrix for a cylinder diameter larger than 1λ and the exact analytical solution is applicable for the other regions (less than 1λ).

ACKNOWLEDGEMENT

This study was supported by the Korea Aerospace Research Institute (KARI).

REFERENCES

- Ruck, G.T., Barric, D.E., Stuart, W.D., Krichbaum, C.K., 1970. *Radar Cross Section Handbook*, Plenum, NY.
- Sarabandi, K., 1989. *Electromagnetic scattering from vegetation canopies*, Ph D. Thesis, Radiation Laboratory, University of Michigan, pp. 190-234.
- Ulaby, F.T., M.K. Moore, and A.K. Fung, 1982. *Microwave Remote Sensing, Active and Passive*, vol.

2, Artech House, Norwood, MA, USA.

Ulaby, F.T., Elachi, C., 1990. *Radar Polarimetry for Geoscience Applications*, Artech House, Norwood, MA, USA, pp. 53-107.

Ulaby, F.T., El-rayes, M.A., 1987. "Microwvae dielectric spectrum of vegetation – part III : Dual-dispersion model," *IEEE Trans. Geosci. Remote Sensing*, vol. 25, pp. 550-557.

Tsang, L., Kong, J.A., Ding, K.H., 2000. *Scattering of Electromagnetic Waves Theories and Applications*, Wiley, pp. 41-45